

LRP2/megalin is required for patterning of the ventral telencephalon

Robert Spoelgen*, Annette Hammes*, Uwe Anzenberger*, Dietmar Zechner, Olav M. Andersen, Boris Jerchow and Thomas E. Willnow†

Max-Delbrueck-Center for Molecular Medicine, Berlin, 13092, Germany

*Authors contributed equally

†Author for correspondence (e-mail: willnow@mdc-berlin.de)

Accepted 10 November 2004

Development 132, 405-414

Published by The Company of Biologists 2005

doi:10.1242/dev.01580

Summary

Megalin is a low-density lipoprotein receptor-related protein (LRP2) expressed in the neuroepithelium and the yolk sac of the early embryo. Absence of megalin expression in knockout mice results in holoprosencephaly, indicating an essential yet unidentified function in forebrain development. We used mice with complete or conditional megalin gene inactivation in the embryo to demonstrate that expression of megalin in the neuroepithelium but not in the yolk sac is crucial for brain development. During early forebrain development, megalin deficiency leads to an increase in bone morphogenic protein (*Bmp*) 4 expression and signaling in the rostral dorsal neuroepithelium, and a subsequent loss of sonic hedgehog (*Shh*) expression in the

ventral forebrain. As a consequence of absent SHH activity, ventrally derived oligodendroglial and interneuronal cell populations are lost in the forebrain of megalin^{-/-} embryos. Similar defects are seen in models with enhanced signaling through BMPs, central regulators of neural tube patterning. Because megalin mediates endocytic uptake and degradation of BMP4, these findings indicate a role for megalin in neural tube specification, possibly by acting as BMP4 clearance receptor in the neuroepithelium.

Key words: LDL receptor-related proteins, Bone morphogenic proteins, Sonic hedgehog, Yolk sac, Holoprosencephaly, Mouse, LRP2

Introduction

Low-density lipoprotein (LDL) receptor-related proteins (LRPs) are multifunctional cell surface receptors structurally related to the LDL receptor (Nykjaer and Willnow, 2002). Initially considered endocytic receptors involved in lipoprotein metabolism, recent studies revealed important roles for LRPs in the regulation of many signaling processes (Nykjaer and Willnow, 2002; Herz and Bock, 2002). For example, LRP5 and LRP6 bind WNT proteins and WNT inhibitors, and act as co-receptors for Frizzled in determining pattern formation in the early embryo (Pinson et al., 2000; Wehrli et al., 2000; Mao et al., 2001a; Mao et al., 2001b), while apolipoprotein E receptor-2 and very low-density lipoprotein receptor function as receptors for Reelin, a signaling factor that controls neuronal migration in the embryonic brain (Trommsdorf et al., 1999; Hiesberger et al., 1999; D'Arcangelo et al., 1999).

LRP2, or megalin (herein referred to as megalin), is another member of the LDL receptor gene family essential for brain development (Saito et al., 1994; Willnow et al., 1996). At mid-gestation, the receptor is expressed in the neuroepithelium of the embryo as well as in the visceral endoderm of the yolk sac (Willnow et al., 1996; Zheng et al., 1994). Targeted disruption of the respective gene in the mouse results in holoprosencephalic syndrome and in perinatal lethality (Willnow et al., 1996). However, the exact mechanism by which megalin contributes to forebrain formation, and why holoprosencephaly (HPE) ensues in megalin-deficient mice, is still unclear.

Holoprosencephaly is defined as a failure of the prosencephalon (forebrain) to separate along the mid-sagittal

axis into discrete hemispheres. This defect is likely to be the result of defective patterning during development involving improper specification of the rostral portion of the neural tube. Many genetic pathways involved in neural tube patterning have been implicated in the etiology of HPE (Wallis and Muenke, 1999). In particular, alterations in pathways that specify the dorsoventral axis of the rostral neural tube may cause this syndrome. For example, increased dorsal signaling through bone morphogenic proteins (BMPs), members of the transforming growth factor β superfamily, and through WNT proteins, results in HPE (Golden et al., 1999; Wallis et al., 1999; Anderson et al., 2002; Lagutin et al., 2003). Also, loss of sonic hedgehog (SHH) expression, a factor that specifies the ventral neural tube, leads to holoprosencephalic syndrome in humans and in mice (Chiang et al., 1996; Roessler et al., 1996).

Concerning a role for megalin in forebrain development, some evidence suggests involvement of the receptor in the SHH pathway (McCarthy et al., 2002; Farese and Herz, 1998). Sonic hedgehog is a secreted protein expressed in the notochord and the floorplate that undergoes autocatalytic cleavage into a 19 kDa amino terminal (SHH-N) and a 25 kDa carboxyl terminal (SHH-C) domain. During cleavage, a cholesterol moiety becomes covalently attached to SHH-N, the active fragment that binds to the receptor Patched (Ptch1) and activates downstream SHH target genes through Smoothed (Smo). Cholesterol modification of SHH-N is crucial for proper activity, perhaps by spatially restricting SHH activity (Porter et al., 1996). Expression of megalin in the yolk sac and its ability to take up lipoproteins suggests a possible function for the receptor in delivery of cholesterol-rich lipoproteins

from the maternal circulation to the embryo for SHH activation (Willnow et al., 1992; Farese and Herz, 1998). Alternatively, expression of megalin in the neuroepithelium and its ability to bind SHH indicates a more direct effect as a co-receptor in SHH signaling (McCarthy et al., 2002).

In the present study, we used mice in which the megalin gene was ubiquitously inactivated (including yolk sac and neuroepithelium) or conditional mutants with loss of megalin only in the neuroepithelium to examine the contribution of the receptor in these tissues to forebrain formation. Sustained expression of megalin in the yolk sac did not rescue mice from HPE, indicating that a receptor activity in the neuroepithelium is essential for normal forebrain development. In the neuroepithelium, megalin activity affects dorsal and ventral patterning of the forebrain, and promotes ventral cell fate specification.

Materials and methods

Animals

The generation of mice with targeted disruption of the megalin gene has been described (Willnow et al., 1996). The megalin gene defect was analyzed in receptor-deficient and in somite-matched wild-type littermates on a hybrid (129SvEmcTer × C57BL/6N) and on an inbred CD1 genetic background. Both lines gave identical results. For conditional inactivation of the megalin gene in the epiblast, animals homozygous for a *loxP*-modified allele of the megalin gene (megalin^{lox/lox}) (Lehste et al., 2003) were crossed with mice carrying a knock-in of the *Cre* transgene into the *mesenchyme homeobox 2* gene locus (*Meox2*^{tm1(cre)Sor}) obtained from Jackson Laboratories (www.JAX.org) (Tallquist and Soriano, 2000). Embryos from breeding of megalin^{lox/wt}/*Meox2*^{tm1(cre)Sor} mice with megalin^{lox/lox} animals were used for phenotypic analysis following genotyping of embryo- or yolk sac-derived tissues.

Histological and immunohistological analysis

Embryos or yolk sac tissues were dissected from pregnant mice at designated time points, fixed overnight in 4% paraformaldehyde in PBS at 4°C, and embedded in paraffin. Routine paraffin sections were cut at 2–10 µm and stained with hematoxylin and eosin (H+E). For immunohistology, sections were incubated with sheep anti-megalin (1:50,000; provided by P. Verroust, INSERM, Paris), mouse anti-β III tubulin (TuJ1) (1:500; BabCO, Richmond, USA), or rabbit anti-phospho-Smad1/5/8 (1:100; Cell Signaling Technology, Beverly, USA) antisera followed by secondary peroxidase- (1:100; Dako, Hamburg, Germany), Cy3- or Cy5-conjugated antibodies (1:400; Jackson ImmunoResearch Laboratories, West Baltimore Pike, USA). Nuclei were counterstained with 1 µM YO-PRO-1 iodide (Molecular Probes, Eugene, USA).

In-situ hybridization

Embryos were dissected and fixed overnight in 4% paraformaldehyde in PBS at 4°C. Further processing of the embryos and whole-mount in-situ hybridization was carried out essentially as described (Hammes et al., 2001). The localization of signals was studied in whole embryos or in plastic sections thereof. Plasmids for generating in-situ probes were kindly provided by W. Birchmeier [MDC, Berlin; *Nkx2.1* (*Titf1* – Mouse Genome Informatics), *Olig2*, *Wnt1*, *Msx1*, *Fgf8*], J. Huelsken (ISREC, Epalinges; *Ptch1*, *Bmp4*, *Wnt7*, *Gli2*, *Gli3*), A. Joyner (Mount Sinai Research Institute, Toronto; *Gli1*), J. L. R. Rubenstein (UCSF, San Francisco; *Dlx2*), A. P. McMahon (Harvard University, Cambridge; *Shh*), and B. Hogan [Vanderbilt University Medical School, Nashville; *Hnf3b* (*Foxa2* – Mouse Genome Informatics)], or generated from first strand mouse cDNA (*Pax6*, *Pax2*, *Smo*, *Plp2*).

Apoptosis and proliferation assays

Embryonic day 10.5 embryos were dissected, fixed, paraffin-embedded and sectioned as described above. After de-waxing and rehydration, the sections were incubated with 20 µg/ml proteinase K in 10 mmol/l Tris/HCl, pH 7.4 for 20 minutes at 37°C. Detection of apoptotic cells was performed using the TUNEL reaction kit (www.Roche.com) following manufacturer's instructions. For detection of proliferation, paraffin sections were incubated with rabbit anti-phosphohistone H3 antibody (1:200; Upstate, Lake Placid) followed by secondary Cy3-conjugated sheep anti-rabbit IgG (Sigma, www.sigma.com), and detection by immunofluorescence microscopy.

BIAcore analysis and cell culture experiments

Carrier-free preparations of recombinant human BMP4 and BMP5 were purchased from Research and Development (www.RnDSystems.com). Recombinant His-tagged RAP was produced and purified from bacteria by standard Ni²⁺ affinity chromatography. As a source for WNT1 we used conditioned medium from Rat-2 cells infected with a retroviral *Wnt1* expression construct that excrete large amounts of the protein (Rat-2/WNT1) and compared it with medium from cells infected with the empty expression vector (Rat-2/MV7) (cell lines kindly provided by A. M. C. Brown, Cornell University, New York) (Giarre et al., 1998). Interaction of megalin with BMP4, BMP5 and RAP (0.5–1 µmol/l) or WNT1 (20-fold concentrated medium) was tested by surface plasmon resonance (SPR) as described before (Hilpert et al., 1999). For cell uptake studies, BMP4 was iodinated according to the IODOGEN protocol (specific activity 3.1 × 10⁸ cpm/µg). Replicate monolayers of rat choriocarcinoma (BN16) cells were incubated for 2 hours with 1.6 ng/ml of ¹²⁵I-BMP4 in the presence of buffer, 200 µmol/l chloroquine, or 100 µg/ml RAP. Degradation of ligand was determined as the total amount of ¹²⁵I-labeled trichloroacetic acid-soluble material released into the culture medium and expressed as picogram ligand per mg of total cell protein (Hilpert et al., 1999).

Results

Megalin deficiency impairs forebrain development around mid-gestation

Mice homozygous for a targeted disruption of the megalin gene suffer from malformations of the forebrain and mid-face structures consistent with features observed in holoprosencephalic syndrome (Willnow et al., 1996). By external inspection, megalin^{-/-} newborns are characterized by severe facial dysgenesis, in particular by a shortened snout and incompletely developed or absent eyes (Fig. 1B). Histological sections of the brain reveal improper separation of the forebrain hemispheres and extended lateral ventricles (Fig. 1D) that may even be fused to a single central cavity (Fig. 1F). In agreement with observations in other models of HPE, the phenotypic features are variable and may include lack of the corpus callosum, absence of the olfactory bulbs and fusion of forebrain hemispheres. Occasionally, phenotypes resembling an exencephalus are observed (Willnow et al., 1996).

To identify the exact time point in development that phenotypic abnormalities are first apparent in megalin-deficient embryos, we characterized earlier developmental stages in this mouse line. At embryonic day (E) 14.5, knockout embryos exhibited a full spectrum of malformations that ranged from enlarged ventricles (Fig. 1H) to exencephalus and a common ventricular system (Fig. 1I). At E12.5, megalin^{-/-} embryos were characterized by a small telencephalon (not shown) and a thin-walled neuroepithelium (Fig. 1M, arrowhead). The reduction in neuroepithelial wall thickness

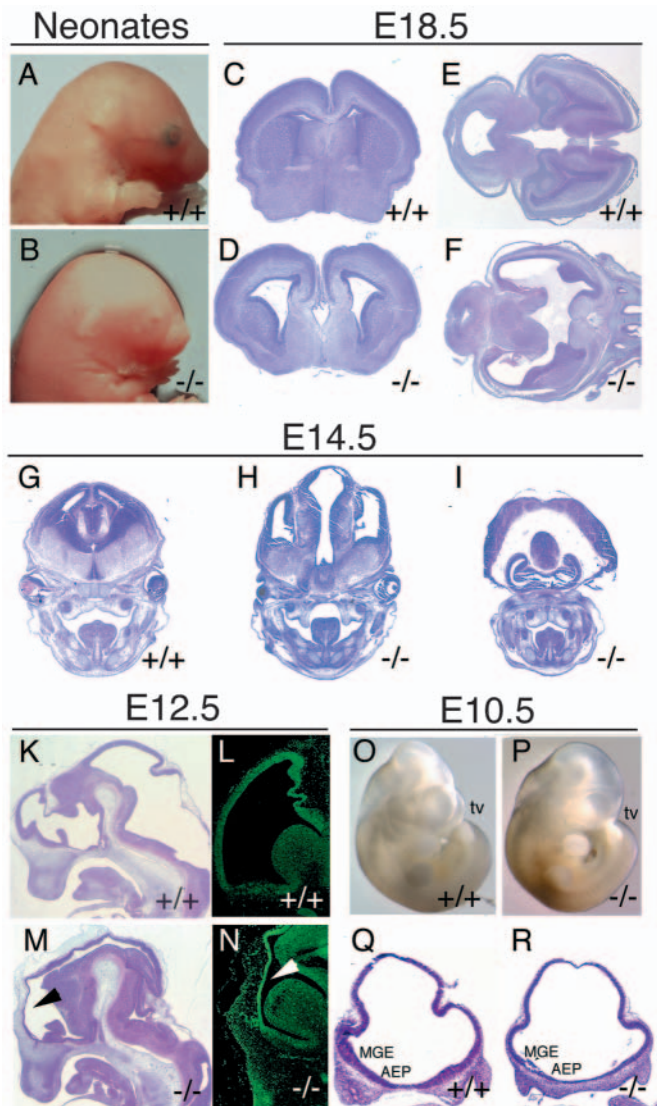


Fig. 1. Neuroanatomy of megalin-deficient neonates and embryos. (A,B) External appearance of wild-type (A) and megalin^{-/-} neonates (B), highlighting craniofacial abnormalities in the receptor-deficient mouse. (C,D) Coronal H+E stained sections through the rostral brain of E18.5 embryos, depicting enlarged ventricles in the megalin-deficient animal (D) compared with the control (C). (E,F) Horizontal sections through the brain at E18.5, demonstrating a single cerebral hemisphere with a central fused ventricle in the megalin^{-/-} embryo (F) compared with bilateral hemispheres with two lateral ventricles in the control (E). (G-I) Coronal forebrain sections of wild-type (G) and megalin^{-/-} E14.5 embryos (H,I), with abnormalities ranging from enlarged ventricles (H) to exencephalus and a common ventricular system (I). (K-N) Sagittal forebrain sections from wild type (K,L) and megalin-deficient E12.5 embryos (M,N) subjected to H+E staining (K,M) or detection of cell death by TUNEL assay (L,N). megalin^{-/-} embryos suffer from a reduction in neuroepithelial wall thickness (M, arrowhead) compared with controls (K) that coincides with massive apoptosis in the roof of the cerebral cortex (N, arrowhead). (O,P) Lateral aspects of wild-type (O) and megalin^{-/-} (P) E10.5 embryos. Note the reduced size of the telencephalic vesicles in the knockout. (Q,R) Coronal forebrain sections, indicating a decrease in thickness of the ventral neuroepithelium that is most pronounced in the AEP and the MGE of megalin^{-/-} embryos (R) compared with megalin^{+/+} embryos (Q). (C-M,O-R: H+E staining). AEP, anterior entopeduncular area; MGE, medial ganglionic eminence; tv, telencephalic vesicles.

coincided with massive induction of cell death that was most prominent in the roof of the neopallium (Fig. 1N, arrowhead). At E10.5, the phenotype of the megalin^{-/-} embryos first became apparent, typically as an overall reduction in size of the telencephalic vesicles (Fig. 1P) and a decrease in neuroepithelial wall thickness that was most pronounced in the anterior entopeduncular area (AEP) and the medial ganglionic eminence (MGE) (Fig. 1R). Otherwise, the embryos appeared normally developed, with a similar body size and external appearance, and an identical number of somites (35-39), to control littermates (Fig. 1O,P). At E9.5 no obvious phenotypic differences in gross morphology were detected in knockout embryos compared with control embryos (data not shown), indicating a time point around mid-gestation when megalin deficiency manifests itself morphologically.

Forebrain defects in mice with epiblast-specific megalin gene disruption

During early development, megalin is expressed in the visceral endoderm of the yolk sac and in the neuroepithelium (Fig. 2A,C). Conceivably, lack of megalin expression in either the

embryonic or the extra-embryonic tissues (or both) may be responsible for the brain malformations in knockout mice. To dissect the contributions of both tissues to the occurrence of forebrain defects, we used conditional gene targeting to inactivate the megalin gene specifically in the embryo proper and retain gene expression in the yolk sac. To do so, we employed a mouse line carrying a megalin gene modified by *loxP* sites (megal^{lox/lox}) that had been used successfully before to achieve tissue-specific receptor gene inactivation (Lehste et al., 2003). megal^{lox/lox} animals were bred with mice carrying the cre recombinase gene under control of the mesenchyme homeobox 2 gene promoter (*Meox2*^{tm1(cre)Sor}), directing *Cre* gene expression to the epiblast (Tallquist and Soriano, 2000). Consistent with this strategy, embryos homozygous for the *loxP*-modified megalin gene and carrying the *Cre* transgene (megal^{lox/lox}/*Meox2*^{tm1(cre)Sor}) lacked expression of the receptor in the neuroepithelium (Fig. 2D) but not in the yolk sac (Fig. 2B). Despite normal expression of megalin in the visceral endoderm of the yolk sac, megal^{lox/lox}/*Meox2*^{tm1(cre)Sor} embryos suffered from similar brain defects to megalin^{-/-} embryos (Fig. 2E,F), demonstrating that megalin activity in the embryo proper is required for brain development.

Altered proliferation in the rostral ventral neural tube of megalin^{-/-} embryos

Forebrain anomalies in megalin-deficient embryos resembled phenotypes seen in models with altered dorsoventral patterning of the rostral neural tube. Therefore, we focused further studies on a role of the receptor in brain development at embryonic stages E9.5 to 10.5, when the forebrain vesicles subdivide. Because *Cre*-mediated inactivation of the megalin gene in the epiblast of megal^{lox/lox}/*Meox2*^{tm1(cre)Sor} embryos was inefficient and yielded few embryos with complete loss of receptor expression in the neuroepithelium, we mainly used

megalin^{-/-} animals for this analysis. However, we confirmed key findings in mice with epiblast-specific receptor gene defect.

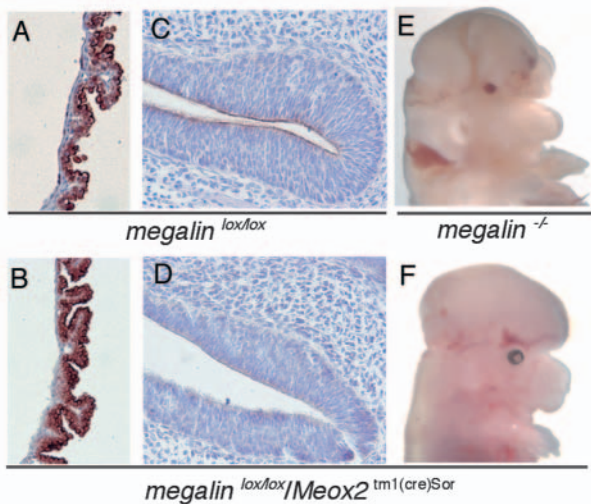


Fig. 2. Forebrain abnormalities and megalin expression pattern in E14.5 embryos with conditional megalin gene inactivation. (A-D) Immunohistological detection of megalin in yolk sac (A,B) and neuroepithelium (C,D) of E14.5 embryos. megalin^{lox/lox} embryos express the receptor in the yolk sac (A) and the neuroepithelium (C), whereas megalin^{lox/lox/Meox2^{tm1(cre)Sor}} embryos express the receptor in the yolk sac (B) but not in the neuroepithelium (D). (E,F) Exencephalus in E14.5 embryos with ubiquitous (megal^{-/-}) (E) or with epiblast-specific (megal^{lox/lox/Meox2^{tm1(cre)Sor}}) megalin gene knockout (F).

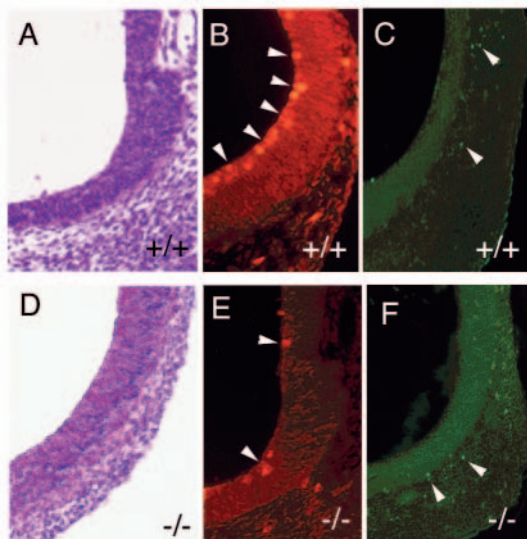


Fig. 3. Analysis of cell proliferation and apoptosis in the neural tube of E10.5 embryos. Coronal sections through the rostral ventral neural tube of wild-type (A-C) and megalin knockout embryos (D-F) stained with H+E (A,D), or analyzed for cell proliferation (B,E) (anti-phosphohistone H3 immunofluorescence) or apoptosis (C,F) (TUNEL assay). The number of mitotic cells is reduced in the rostroventral neural tube of the megalin^{-/-} embryo (E, arrowheads) compared with the control (B, arrowheads). No difference is seen in the number of apoptotic nuclei in both genotypes (C,F; arrowheads).

Given the reduction in neuroepithelial wall thickness in knockout embryos (Fig. 1R), we first analyzed mitotic activity in this tissue. Decreased proliferation was observed in a restricted area of the rostral ventral neural tube, as evidenced by the number of nuclei that stained positive for phosphohistone (8.3 ± 1.1 SD versus 22.7 ± 2 SD mitotic cells per microscopic field; $P=0.001$; $n=3$ animals for each genotype) (Fig. 3B,E). Other areas of the neural tube were not affected (data not shown). Furthermore, TUNEL assays did not reveal any discernable difference in the number of apoptotic cells at E10.5 in the ventral neuroepithelium (5.0 ± 0.5 SD versus 4.7 ± 0.6 SD apoptotic nuclei per microscopic field, $P=0.64$) (Fig. 3C,F) or the dorsal neuroepithelium (not shown).

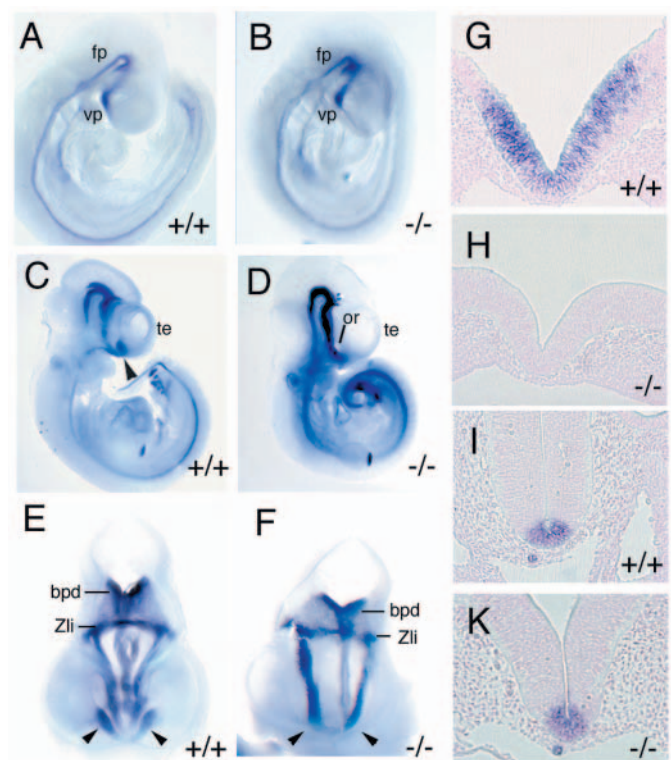


Fig. 4. *Shh* expression in wild-type and megalin^{-/-} embryos. (A,B) Whole-mount in-situ hybridization (ISH) in E9.5 wild type (A) and megalin-deficient embryos (B), demonstrating an identical expression pattern for *Shh* in floorplate and ventral prosencephalon. (C,D) Whole-mount ISH for *Shh* in E10.5 embryos, indicating expression in the ventral telencephalon of the wild type (C, arrowhead) but not in the ventral telencephalic region anterior to the optic recess of megalin^{-/-} embryos (D). (E,F) Frontal head aspects of wild type (E) and megalin^{-/-} E10.5 embryos (F), depicting *Shh* expression in the AEP (arrowheads) of wild-type but not knockout animals. Expression of *Shh* in other areas of the forebrain, such as in the basal plate of the diencephalon (bpd) or the zona limitans intrathalamica, is identical in both. (G-K) ISH for *Shh* on coronal sections of the rostral (G,H) and the caudal (I,K) neural tube. *Shh* is expressed in the AEP of the rostroventral neural tube of wild-type (G) but not megalin^{-/-} E10.5 embryos (H), while expression in caudal regions of the neural tube is identical in wild-type (I) and knockout tissues (K). bpd, basal plate of the diencephalon; fp, floorplate; or, optic recess; te, telencephalon; vp, ventral prosencephalon; Zli, Zona limitans intrathalamica.

Absence of *Shh* expression in the AEP of megalin^{-/-} embryos

Because SHH stimulates proliferation of cell populations in the rostral ventral forebrain, we tested for alterations in the expression of this morphogen as a possible reason for the defects in megalin-deficient embryos. At E9.5, *Shh* is expressed in the notochord, floorplate and ventral prosencephalon. No differences in this pattern were seen when comparing wild-type and knockout embryos (Fig. 4A,B). However, the situation changed at E10.5. While expression of *Shh* in most embryonic tissues, including notochord, floorplate, limb buds and ventral diencephalon, was unaffected in megalin^{-/-} embryos, specific loss of the *Shh* signal in the ventral region of the telencephalon anterior to the optic recess was observed (Fig. 4C,D). By close inspection of frontal head aspects, the *Shh* signal lacking in megalin knockout embryos localized to a region of the ventral neural tube in wild types defined as the AEP (Fig. 4E, arrowheads). In other regions of the forebrain such as the basal plate of the diencephalon (bpd) and the zona limitans intrathalamica (Zli), *Shh* expression was identical in wild types and knockouts (Fig. 4E,F). This finding was substantiated on coronal brain sections indicating locally restricted loss of *Shh* expression in the AEP (Fig. 4H) but not in other *Shh* expression domains in the ventral neural tube of knockout embryos (Fig. 4K). Specific loss of *Shh* expression in the AEP was also confirmed in mice with epiblast-specific receptor gene defect (Fig. 5C,D). In wild types, co-expression

of megalin and *Shh* was observed in neuroepithelial cells in this tissue (Fig. 6).

Loss of ventral cell fate in the telencephalon of megalin-deficient embryos

SHH activity is essential to induce proliferation and differentiation of specific cell populations in the progenitor zone of the ventral neural tube (Marin and Rubenstein, 2001; Nery et al., 2001; Fuccillo et al., 2004). SHH signaling is particularly required for the development of oligodendrocyte precursors that originate from the AEP and migrate tangentially into adjacent areas of the forebrain to develop into myelin-forming glia (Marin and Rubenstein, 2001). As seen by in-situ hybridization (ISH) for the mRNA encoding oligodendrocyte transcription factor 2 (*Olig2*), an early marker of the oligodendroglial lineage, expression of *Olig2* in E10.5 wild-type embryos paralleled the pattern for *Shh* expression in the AEP (Fig. 7A). By contrast, little *Olig2* signal was observed in this tissue of megalin^{-/-} embryos, while expression in the thalamus region of the diencephalon was normal (Fig. 7A). Similar findings were obtained for myeloid proteolipid protein (*Plp1*), another oligodendrocyte marker gene (data not shown).

We also explored the consequence of *Shh* deficiency on the generation of neuronal precursor populations that arise in the AEP and MGE, applying ISH for marker genes highly expressed in these cell types at E10.5 (Sussel et al., 1999; Marin et al., 2000; Fuccillo et al., 2004). The *Shh*-dependent homeobox gene *Nkx2.1* is essential for the production of basal forebrain cholinergic neurons and cortical interneurons (Sussel et al., 1999). *Dlx2*, another SHH-dependent homeobox gene, specifies cells that originate in the ventral telencephalon and migrate tangentially to populate the cerebral cortex, olfactory bulb and hippocampus, where they differentiate into interneurons (Corbin et al., 2001). As shown in Fig. 7B, no expression of *Nkx2.1* was detected in the ventral telencephalon of megalin-deficient animals, while expression in other forebrain regions, such as the thalamus of the diencephalon,

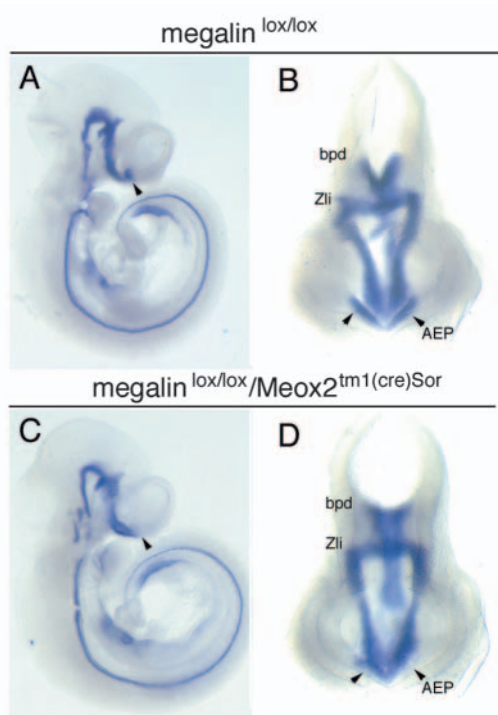


Fig. 5. *Shh* expression in megalin^{lox/lox} and megalin^{lox/lox}/*Meox2*^{tm1(cre)Sor} E10.5 embryos. (A,C) Lateral and (B,D) frontal head aspects of whole-mount in-situ hybridization for *Shh* in E10.5 embryos, indicating expression in the AEP of megalin^{lox/lox} (A,B; arrowheads) but not megalin^{lox/lox}/*Meox2*^{tm1(cre)Sor} embryos (C,D, arrowheads). bpd, basal plate of the diencephalon; Zli, zona limitans intrathalamica.

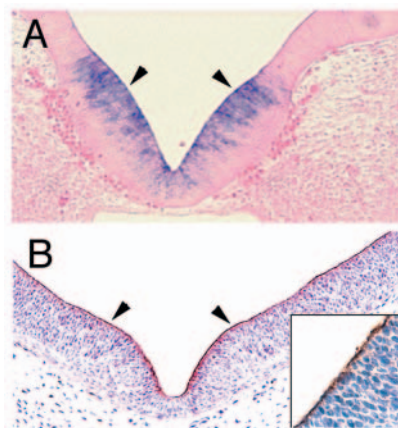


Fig. 6. Co-expression of *Shh* and megalin in the AEP of E10.5 embryos. In-situ hybridization for *Shh* (A) and immunohistology for megalin (B) on coronal sections of the rostroventral neural tube of wild-type E10.5 embryos identify co-expression in the AEP (arrowheads). The inset highlights localization of megalin protein on the apical surface of neuroepithelial cells.

was normal. Also, expression of *Dlx2* was absent in the ventral telencephalon and significantly decreased in the thalamus of E10.5 megalin^{-/-} embryos (Fig. 7C). Specific loss of ventral

neuronal cell populations was confirmed by the lack of neuron-specific class III β -tubulin (TuJ1) signals in the ventral, but not in the dorsal, telencephalon of megalin-deficient animals (Fig. 7D).

So far our results had uncovered an obvious effect of megalin deficiency on the specification of ventral cell fate in the rostral ventral forebrain, probably due to locally restricted loss of *Shh* in the AEP. Consistent with normal expression of *Shh* in areas of the forebrain other than the AEP, the expression patterns of the receptor *Ptch1* (Fig. 7E), the signaling component *Smo* (not shown), or global *Shh* target genes *Hnf3b* (Fig. 7F), *Gli1*, *Gli2* or *Gli3* (not shown) were unchanged in megalin knockout mice.

Altered dorsal telencephalic patterning in megalin^{-/-} mice

Given the loss of ventral *Shh*-dependent pathways in megalin^{-/-} embryos, we also tested whether expression of dorsal markers of the developing brain may be deranged in receptor-deficient mice. *Wnt1*, a marker of early forebrain development, is expressed in the dorsal midline of the di- and mesencephalon, and in the isthmus of wild types at E10.5. No difference in expression patterns of WNT1 (Fig. 7G) or another WNT ligand, WNT7 (data not shown), was seen in knockouts, suggesting normal dorsal patterning of the diencephalon. However, the situation was different when evaluating dorsal markers also found in the telencephalon. *Pax6* is normally expressed in the dorsal part and ventral thalamus of the diencephalon, and the eyes, as well as in the dorsal telencephalon (Fig. 7H). By contrast, in E10.5 megalin^{-/-} embryos *Pax6* expression significantly extended from dorsal areas into ventral areas of the telencephalic neural tube, while expression in the optic vesicles was mostly lost (Fig. 7H).

Enhanced *Bmp4* signaling and aberrant *Fgf8* expression in the dorsal midline of megalin^{-/-} mice

Fibroblast growth factor (*Fgf*) 8 and bone morphogenic protein (BMP) 4 are morphogens that also play key roles in dorsoventral patterning of the rostral head and that act in precise synergy with SHH to maintain normal prosencephalic development (Schneider et al., 2001; Ohkubo et al., 2002). Intriguingly, expression of both morphogens was also significantly altered in mice lacking megalin.

At E10.5, the expression of *Fgf8* was reduced in the rostral ventral telencephalon but extended from the commissural plate along the midline into more dorsal and caudal regions of the forebrain (Fig. 8A). *Bmp4*, demarcating dorsal midline structures, was also aberrantly expressed at E10.5. In wild types, *Bmp4* expression was restricted to the dorsomedial part of the telencephalon and the dorsal midline of the most anterior diencephalon (Fig. 8B). In mutants, expression in the dorsomedial neuroepithelium of the tel- and diencephalon was significantly increased and extended along the midline into more caudal regions of the roof (Fig. 8B, arrowhead). *Bmp4* overexpression in megalin-deficient embryos resulted in enhanced and ventrally expanded BMP4 signaling in the prosencephalon but not in other areas of the neural tube (such as the spinal cord), as shown by immunodetection of phosphorylated Smad proteins (P-Smad) (Fig. 8C). Similar changes in *Bmp4* and *Fgf8* signals were also seen in E10.5

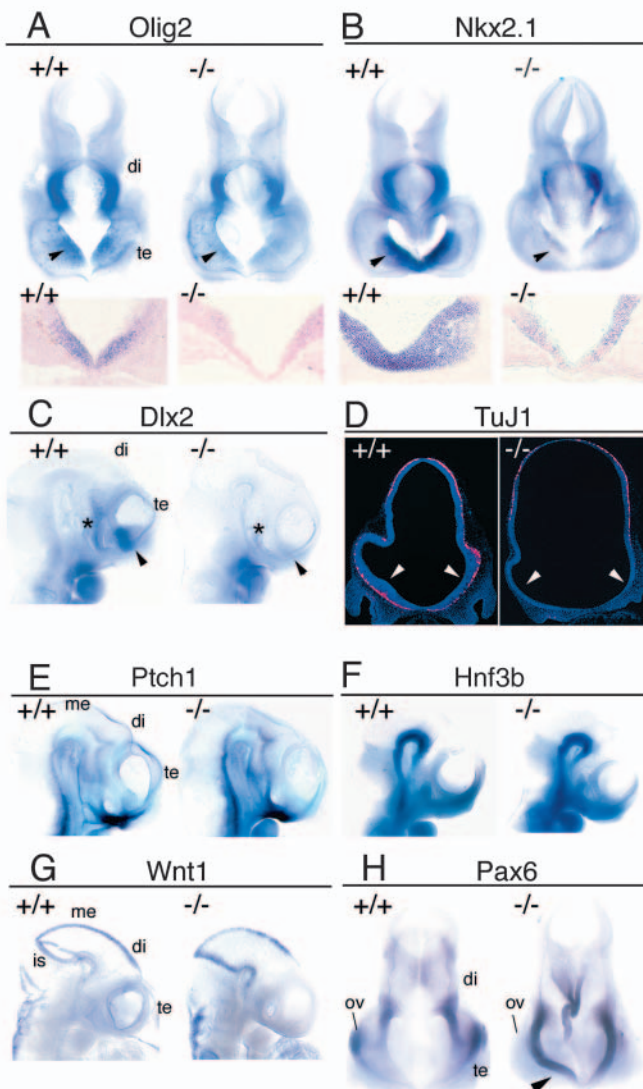
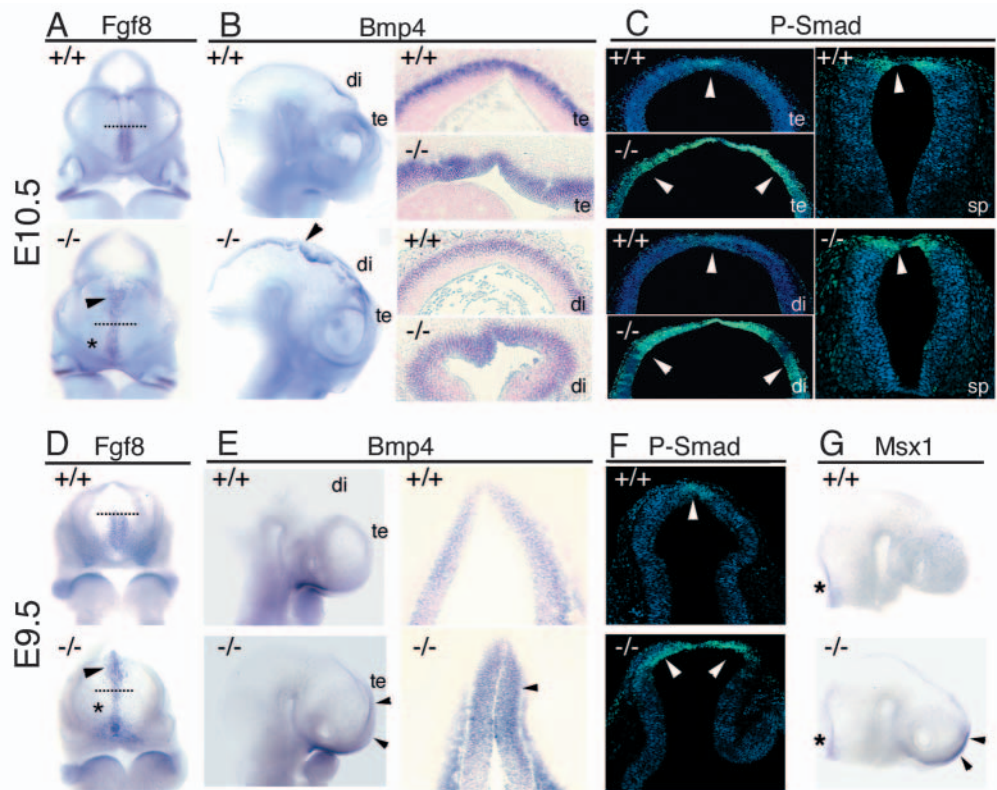


Fig. 7. Expression of marker genes of early forebrain development in E10.5 embryos. (A,B) In-situ hybridization (ISH) of frontal head aspects (upper panel) and coronal forebrain sections (lower panel) demonstrate reduced signals for *Olig2* (A) and *Nkx2.1* (B) in the AEP (arrowheads) but not in the diencephalon of megalin^{-/-} embryos. (C) Expression of *Dlx2* is lost in the ventral telencephalon (arrowheads) and significantly reduced in the ventral thalamus region of the diencephalon (asterisks) of megalin^{-/-} embryos as shown by whole-mount ISH. (D) Immunohistochemistry of coronal E10.5 forebrain sections indicate lack of TuJ1 expression in the ventral (arrowheads), but not in the dorsal, telencephalic region of megalin^{-/-} compared with control embryos. (E-H) Using whole-mount ISH, no differences can be seen in the expression patterns of *Ptch1* (ventral neural tube, including tel-, di- and mesencephalon) (E), *Hnf3b* (ventral neural tube, including di- and mesencephalon) (F), or *Wnt1* (roof of di- and mesencephalon, isthmus) (G), whereas expression of *Pax6* extends from the dorsal into the ventral neural tube of receptor-deficient embryos (H, arrowhead). Also, most knockouts lack the *Pax6* signal in the optic vesicle. di, diencephalon; is, isthmus; me, mesencephalon; ov, optic vesicle; te, telencephalon.

Fig. 8. Analysis of *Fgf8* and *Bmp4* pathways in E9.5 and E10.5 embryos. (A) Anteroventral head aspects of E10.5 embryos, demonstrating a reduction of *Fgf8* expression in the ventral telencephalon (asterisk) and an extension from the commissural plate (dotted line) into more dorsal regions of the midline (arrowhead) in megalin-deficient animals. (B) In-situ hybridization of lateral head aspects (left panel) *Bmp4* expression in wild types is restricted to the dorsomedial part of the telencephalon and the dorsal midline of the most anterior diencephalon, whereas in megalin mutants the *Bmp4* expression domain extends along the midline into more caudal regions of the roof (arrowhead). Coronal sections (right panel) highlight increased *Bmp4* signals in the telencephalon and the anterior diencephalon of knockout compared with control embryos. (C) Immunodetection of P-Smad proteins, indicating a signal in E10.5 wild types that is restricted to the dorsal midline of the tel- and diencephalon (arrowheads) but that is significantly enhanced and ventrally expanded (arrowheads) in megalin^{-/-} littermates. P-Smad signals in the spinal cord are identical in both genotypes. (D) At E9.5, the *Fgf8* expression domain in megalin^{-/-} animals is reduced in the ventral (asterisk), but extended into the dorsal, region of the telencephalon (arrowhead). (E-G) At E9.5, expression of *Bmp4* is increased in the rostral and dorsal telencephalon (arrowheads) of megalin^{-/-} embryos as shown by whole-mount ISH (E, left panel) or coronal dorsal forebrain sections thereof (E, right panel). Increases in *Bmp4* message result in enhanced phosphorylation of Smad proteins (F, arrowheads) and induced expression of *Bmp4* target gene *Msx1* in the rostral dorsal telencephalon (G, arrowheads). *Msx1* expression in the hindbrain region is unchanged (asterisks). di, diencephalon; sp, spinal cord; te, telencephalon.



embryos with epiblast-specific receptor gene defect (data not shown).

Contrary to the findings obtained with *Shh* (Fig. 4A,B), alterations in *Bmp4* and *Fgf8* pathways were already evident at E9.5 in megalin^{-/-} embryos. Thus, the expression domain of *Fgf8* was reduced in the ventral but increased along the dorsal telencephalic midline (Fig. 8D), while expression of *Bmp4* was significantly enhanced in the rostral dorsal telencephalon (Fig. 8E). Again, enhanced BMP4 signaling in the forebrain was confirmed by a concomitant rise and ventral expansion of P-Smad proteins along the rostral neuroepithelial midline (Fig. 8F) and by an aberrantly strong induction of the *Bmp4* target gene *Msx1* in this region (Fig. 8G).

Megalin acts as an endocytic receptor for BMP4

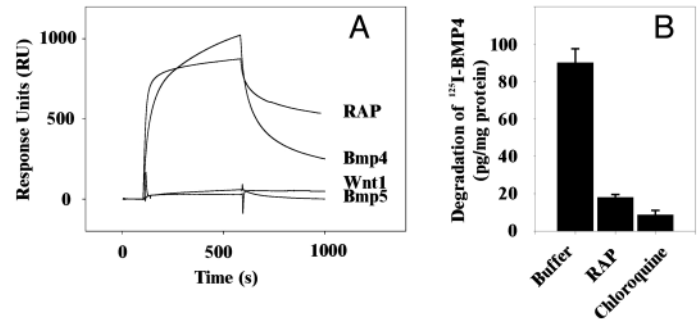
Based on the distinct alterations in SHH and BMP4-dependent pathways in the neural tube of megalin-deficient embryos, a direct involvement of this receptor in the activity of either morphogen seems plausible. The ability of megalin to bind SHH has been reported before (McCarthy et al., 2002). To also establish a potential role for this receptor in BMP4 signaling, we tested the interaction of the receptor with BMP4 by surface plasmon resonance (SPR) analysis. In this assay, BMP4 strongly bound to megalin, while the related factor BMP5 or WNT1 did not (Fig. 9A), suggesting a possible function for

megalin as BMP4 receptor in the early forebrain. Exposure of megalin-expressing (BN16) cells to radiolabeled BMP4 resulted in endocytic uptake and lysosomal degradation of the protein (Fig. 9B). The cellular catabolism of BMP4 was mediated by megalin, because uptake and degradation of ¹²⁵I-BMP4 was blocked completely by the megalin antagonist receptor-associated protein (RAP) (Christensen et al., 1992; Hilpert et al., 1999) and by chloroquine, an inhibitor of lysosomal degradation (Fig. 9B). Taken together, these findings indicated a possible function of megalin as BMP4 clearance receptor in the neuroepithelium and increased BMP signaling in the forebrain as a consequence of the megalin gene defect.

Discussion

We have explored the function of megalin as a regulator of forebrain development using knockout mouse models. Lack of the receptor results in defects in SHH and BMP4 pathways in the neural tube and in impaired establishment of ventral cell fate, particularly affecting oligodendroglial and interneuronal cell populations. The similarities between megalin knockout mice and animal models with altered SHH or BMP4 activities in the forebrain indicate a crucial role for this receptor in morphogen pathways that specify early dorsoventral patterning of the prosencephalon.

Fig. 9. Megalin mediates binding and cellular catabolism of BMP4. (A) Surface plasmon resonance (SPR) analysis of binding of 0.5 $\mu\text{mol/l}$ BMP4 but not of 0.5 $\mu\text{mol/l}$ BMP5 or WNT1-conditioned medium to purified megalin immobilized on the sensor chip surface (see Materials and methods for details). As a positive control, binding of 1 $\mu\text{mol/l}$ receptor-associated protein (RAP) to megalin was tested. (B) Megalin-expressing BN16 cells mediate uptake and lysosomal degradation of ^{125}I -BMP4. Degradation of BMP4 can be blocked by chloroquine (200 $\mu\text{mol/l}$) or the receptor-antagonist RAP (100 $\mu\text{g/ml}$).



The role of megalin in forebrain development: yolk sac or neuroepithelium

Previously, deficiency for megalin in the yolk sac and/or in the neuroepithelium was held responsible for the holoprosencephalic symptoms in megalin^{-/-} mice (Willnow et al., 1996; Farese and Herz, 1998; McCarthy and Argraves, 2003). Using Cre-mediated conditional gene inactivation, we generated a mouse line with loss of megalin in the embryo but not in the yolk sac. Surprisingly, restored expression of megalin in the yolk sac did not prevent forebrain malformation (Fig. 2F). The limited number of megalin^{lox/lox}/Meox2^{tm1(cre)}Sor embryos available ($n=15$) precluded a detailed comparison of the phenotypes of mice with complete and with epiblast-specific megalin gene deletion. Therefore, we cannot exclude the fact that some phenotypic differences exist in forebrain abnormalities in these two lines that reflect the influence of megalin in the yolk sac on neural tube formation. However, similar alterations in *Fgf8*, *Shh* and *Bmp4* expression in both lines strongly suggest that megalin deficiency in the neuroepithelium is the main cause of the observed forebrain defects.

Megalin deficiency impairs SHH-dependent ventral cell fate

While the role of megalin in the yolk sac still awaits elucidation, experimental evidence in this study identified the contribution of this receptor in the neuroepithelium to specification of dorsal and ventral signaling pathways in the anterior neural tube. Axial patterning of the neural tube is controlled by secreted factors that have distinct expression domains in the rostral forebrain. In particular, an intricate balance of the morphogens SHH and BMP4 is crucial for specifying dorsoventral forebrain patterning (Sasai and De Robertis, 1997; Ohkubo et al., 2002).

Sonic hedgehog activity defines the ventral neural tube and establishes ventral neuronal and oligodendroglial cell populations (Marin and Rubenstein, 2001; Nery et al., 2001; Rowitch et al., 1999; Lu et al., 2000). Inactivation of the *Shh* gene in the mouse causes defective axial patterning, cyclopia and absence of ventral cell types (Chiang et al., 1996). Surprisingly, lack of megalin results in loss of *Shh* expression specifically in the AEP, whereas expression in further caudal regions of the neural tube is not affected (Fig. 4). The identical phenotype is seen in other models of abnormal dorsoventral patterning and HPE, in particular in those with increased BMP4 activity, as discussed below. Why some defects impair *Shh* activity exclusively in the AEP is unclear at present, but region-specific differences in the molecular mechanism of

SHH action in the rostral forebrain compared with more caudal regions, such as the spinal cord, have been clearly established (Dale et al., 1997). The spatially restricted loss of SHH in the AEP may explain why no overt changes in some components of the global *Shh* signaling pathway (e.g. *Gli1-2*, *Hnf3b*) are detectable in megalin^{-/-} embryos at E10.5, and why some defects in *Shh* knockout mice (such as absence of distal limb structures) are not shared by megalin-deficient animals.

In the AEP, the *Shh* signal peaks around E10.5, when it overlaps with *Olig2* and *Nkx2.1*, markers of oligodendroglial and neuronal lineages, respectively (Fig. 7). Ectopic expression of *Shh* locally induces differentiation of oligodendrocytes from ventral neuroepithelial precursors (Nery et al., 2001), a process blocked by anti-SHH antibodies (Orentas et al., 1999). Consistent with loss of *Shh* in the AEP, megalin-deficient embryos suffer from impaired establishment of neuroepithelial progenitors and from a dramatic reduction in oligodendroglial and interneuronal cell populations, as demonstrated by almost complete absence of *Olig2*, *Nkx2.1*, *Dlx2* and TuJ1-positive cells in the ventral (but not in the dorsal) forebrain (Fig. 7). Potentially, lack of proliferation, increased cell death or impaired differentiation may be held responsible for the absence of ventral cell fate specification. Decreased mitotic activity can be detected in the AEP of megalin^{-/-} embryos; thus, this effect clearly contributes to forebrain anomalies in this mouse line. However, the absence of proliferative defects in other areas of the rostral forebrain and the normal expression of many ventral marker genes (e.g. *Ptch1*, *Smo*, *Hnf3b*, *Gli1*, *Gli2*) strongly suggest that alterations in SHH-dependent differentiation processes also play a causative role. This hypothesis is in agreement with recent findings in which SHH signaling was disrupted in the ventral telencephalon of mice at E9.5 using conditional targeting of the *Smo* gene. Spatial and temporary specific ablation of ventral SHH activity resulted in a complete absence of oligodendrocytes and interneurons in the ventral forebrain, due to impaired differentiation rather than altered proliferation or apoptosis of progenitor cells (Fuccillo et al., 2004).

Megalin deficiency increases BMP4 activity in the rostral dorsal neural tube

Whereas SHH specifies ventral cell fate, BMPs provide inductive signals for dorsal cell types such as the astroglial lineage (Liem et al., 1995; Gross et al., 1996; Timmer et al., 2002). They act through suppression of cell proliferation and induction of apoptosis (Furuta et al., 1997), and function as potent antagonists of the ventral neural tube by blocking SHH action on dorsal cell types and by inhibiting ventral cell fate

(McMahon et al., 1998; Liem et al., 2000). Consistent with an opponent action of dorsal and ventral signaling pathways in the neural tube, increased activity of BMPs suppresses expression of *Shh* in the rostral ventral neuroepithelium. For example, when beads soaked with recombinant BMP4 or BMP5 are implanted into the neural tube of the chicken forebrain, loss of *Shh* expression in the ventral forebrain is observed to cause cyclopia and HPE (Golden et al., 1999). In mice genetically deficient for *noggin*, a BMP4 antagonist, expression of dorsal cell fates is normal but *Shh*-dependent ventral cell fate is lost progressively (McMahon et al., 1998). Finally, in mice homozygous for the deletion of *chordin* and heterozygous for the *noggin* gene defect, deficiencies of both BMP antagonists also cause loss of *Shh* expression, specifically in the AEP, and holoprosencephalic syndrome, a phenotype highly reminiscent of defects in megalin^{-/-} embryos (Anderson et al., 2002).

As well as with alterations in *Bmp4* and *Shh* pathways, megalin-deficient embryos also present with changes in expression of *Fgf8* and *Pax6*. *Fgf8* promotes rather than induces rostroventral telencephalic fate (Wilson and Houart, 2004), and its expression is considered to be dependent on coordinated *Shh* and *Bmp* signaling (Ohkubo et al., 2002). Therefore reduction in ventral *Fgf8* gene expression and the extension of the signal along the dorsal midline probably reflects secondary alterations in dorsoventral patterning of the forebrain and abnormalities in formation of midline tissue. Similarly, the expansion of *Pax6* into ventral parts of the telencephalon of receptor-deficient mice is probably a consequence of absence of SHH in the AEP, as described for other models with specific loss of *Shh* expression in the rostral forebrain (Huh et al., 1999; Gofflot et al., 1999).

The role of megalin in patterning of the rostral neural tube: a working model

What may be the mechanism whereby megalin affects dorsoventral specification of the neural tube? Given the competing action of dorsal and ventral signaling factors on neural tube patterning one may envision two scenarios. In one model, the receptor may be essential to induce *Shh* expression in cells of the AEP and its absence results in loss of SHH activity and in impaired ventral cell fate. Thus, overexpression of the dorsal markers such as BMP4 would be a consequence of the lack of ventral SHH signals. In an alternative model, megalin may act as a negative regulator of *Bmp4* activity in the dorsal neuroepithelium and receptor deficiency causes an increase in dorsal BMP4 signals, an effect known to suppress *Shh* (Golden et al., 1999; McMahon et al., 1998; Liem et al., 2000). Based on the fact that increases in *Bmp4* expression and signaling through phosphorylated Smad proteins at E9.5 clearly precede defects observed in *Shh* at E10.5, we favor the latter model.

A role of megalin in suppression of *Bmp4* expression is supported by findings obtained in this study and by work from others. In the early forebrain, BMP4 is believed to induce its own expression via a positive feedback loop; thus, increases in BMP4 activity are expected to induce *Bmp4* transcription (Blitz et al., 2000). Furthermore, the importance of restricting BMP signals during development is well established and several mechanisms have evolved to negatively regulate morphogen action, including soluble BMP antagonists and dominant negative pseudo-receptors (Balemans and Van Hul, 2002; Onichtchouck et al., 1999). Taken together with the

ability of megalin to catabolize BMP4 (Fig. 9), these findings provide an explanatory model in which megalin acts as an endocytic receptor for BMP4 in the neural tube, antagonizing morphogen signaling. As a consequence of receptor deficiency, BMP4 activity may be locally increased, causing activation of *Bmp4* transcription and stimulation of rostral and dorsal patterning and suppression of ventral patterning. A similar function for megalin as a clearance receptor for parathyroid hormone (PTH) suppressing signaling via the PTH receptor in the kidney has been documented before (Hilpert et al., 1999). Few established cell lines express the receptor megalin, and BN16 cells are the system of choice for testing megalin-dependent endocytosis. The lack of expression of BMP receptors in BN16 cells (R.S., unpublished) currently precludes directly testing the consequence of megalin activity on BMP signaling in these cells. Therefore, future efforts should be directed toward establishing suitable cellular systems (e.g. neural tube explants) to address this question.

In conclusion, our studies have uncovered an important novel activity of LRP6 as modifiers of BMP4- and SHH-dependent patterning of the forebrain, and the role that is played by megalin in this process. These findings have identified megalin as an important factor in axial embryonic pattern formation and characterized a novel molecular pathway that contributes to abnormal specification of the ventral forebrain and to HPE, the most common developmental brain anomaly in humans (Wallis and Muenke, 1999).

We are indebted to C. Raeder, S. Schuetz and J. Zenker for expert technical assistance, and to T. Mueller and W. Birchmeier for helpful discussions. Studies presented here were funded by grants from the DFG and the BMBF.

References

- Anderson, R. M., Lawrence, A. R., Stottmann, R. W., Bachiller, D. and Klingensmith, J. (2002). Chordin and noggin promote organizing centers of forebrain development in the mouse. *Development* **129**, 4975-4987.
- Balemans, W. and van Hul, W. (2002). Extracellular regulation of BMP signaling in vertebrates: a cocktail of modulators. *Dev. Biol.* **250**, 231-250.
- Blitz, I. L., Shimmi, O., Wunnenberg-Stapleton, K., O'Connor, M. B. and Cho, K. W. (2000). Is chordin a long-range- or short-range-acting factor? Roles for BMP1-related metalloproteases in chordin and BMP4 autofeedback loop regulation. *Dev. Biol.* **223**, 120-138.
- Chiang, C., Litingtung, Y., Lee, E., Young, K. E., Corden, J. L., Westphal, H. and Beachy, P. A. (1996). Cyclopia and defective axial patterning in mice lacking Sonic hedgehog gene function. *Nature* **383**, 407-413.
- Christensen, E. I., Moskaug, J. O., Vorum, H., Gundersen, T. E., Nykjaer, A., Blomhoff, R., Willnow, T. E. and Moestrup, S. K. (1999). Evidence for an essential role of megalin in transepithelial transport of retinol. *J. Am. Soc. Nephrol.* **10**, 685-695.
- Corbin, J. G., Nery, S. and Fishell, G. (2001). Telencephalic cells take a tangent: non-radial migration in the mammalian forebrain. *Nat. Neurosci.* **4**, 1177-1182.
- D'Arcangelo, G., Homayouni, R., Keshvara, L., Rice, D. S., Sheldon, M. and Curran, T. (1999). Reelin is a ligand for lipoprotein receptors. *Neuron* **24**, 471-479.
- Dale, J. K., Vesque, C., Lints, T. J., Sampath, T. K., Furley, A., Dodd, J. and Placzek, M. (1997). Cooperation of BMP7 and SHH in the induction of forebrain ventral midline cells by prechordal mesoderm. *Cell* **90**, 257-269.
- Farese, R. V., Jr and Herz, J. (1998). Cholesterol metabolism and embryogenesis. *Trends Genet.* **14**, 115-120.
- Fuccillo, M., Rallu, M., McMahon, A. P. and Fishell, G. (2004). Temporal requirement for hedgehog signaling in ventral telencephalic patterning. *Development* **131**, 5031-5040.
- Furuta, Y., Piston, D. W. and Hogan, B. L. (1997). Bone morphogenetic

- proteins (BMPs) as regulators of dorsal forebrain development. *Development* **124**, 2203-2212.
- Giarre, M., Semenov, M. V. and Brown, A. M.** (1998). Wnt signaling stabilizes the dual-function protein beta-catenin in diverse cell types. *Ann. N. Y. Acad. Sci.* **857**, 43-55.
- Gofflot, F., Kolf-Clauw, M., Clotman, F., Roux, C. and Picard, J. J.** (1999). Absence of ventral cell populations in the developing brain in a rat model of the Smith-Lemli-Opitz syndrome. *Am. J. Med. Genet.* **87**, 207-216.
- Golden, J. A., Bracilovic, A., McFadden, K. A., Beesley, J. S., Rubenstein, J. L. and Grinspan, J. B.** (1999). Ectopic bone morphogenetic proteins 5 and 4 in the chicken forebrain lead to cyclopia and holoprosencephaly. *Proc. Natl. Acad. Sci. USA* **96**, 2439-2444.
- Gross, R. E., Mehler, M. F., Mabie, P. C., Zang, Z., Santschi, L. and Kessler, J. A.** (1996). Bone morphogenetic proteins promote astroglial lineage commitment by mammalian subventricular zone progenitor cells. *Neuron* **17**, 595-606.
- Hammes, A., Guo, J. K., Lutsch, G., Leheste, J. R., Landrock, D., Ziegler, U., Gubler, M. C. and Schedl, A.** (2001). Two splice variants of the Wilms' tumor 1 gene have distinct functions during sex determination and nephron formation. *Cell* **106**, 319-329.
- Herz, J. and Bock, H. H.** (2002). Lipoprotein receptors in the nervous system. *Annu. Rev. Biochem.* **71**, 405-434.
- Hiesberger, T., Trommsdorff, M., Howell, B. W., Goffinet, A., Mumby, M. C., Cooper, J. A. and Herz, J.** (1999). Direct binding of Reelin to VLDL receptor and ApoE receptor 2 induces tyrosine phosphorylation of disabled-1 and modulates tau phosphorylation. *Neuron* **24**, 481-489.
- Hilpert, J., Nykjaer, A., Jacobsen, C., Wallukat, G., Nielsen, R., Moestrup, S. K., Haller, H., Luft, F. C., Christensen, E. I. and Willnow, T. E.** (1999). Megalin antagonizes activation of the parathyroid hormone receptor. *J. Biol. Chem.* **274**, 5620-5625.
- Huh, S., Hatini, V., Marcus, R. C., Li, S. C. and Lai, E.** (1999). Dorsal-ventral patterning defects in the eye of BF-1-deficient mice associated with a restricted loss of shh expression. *Dev. Biol.* **211**, 53-63.
- Lagutin, O. V., Zhu, C. C., Kobayashi, D., Topczewski, J., Shimamura, K., Puelles, L., Russell, H. R., McKinnon, P. J., Solnica-Krezel, L. and Oliver, G.** (2003). Six3 repression of Wnt signaling in the anterior neuroectoderm is essential for vertebrate forebrain development. *Genes Dev.* **17**, 368-379.
- Leheste, J. R., Melsen, F., Wellner, M., Jansen, P., Schlichting, U., Renner-Muller, I., Andreassen, T. T., Wolf, E., Bachmann, S., Nykjaer, A. and Willnow, T. E.** (2003). Hypocalcemia and osteopathy in mice with kidney-specific megalin gene defect. *FASEB J.* **17**, 247-249.
- Liem, K. F., Jr, Tremml, G., Roelink, H. and Jessell, T. M.** (1995). Dorsal differentiation of neural plate cells induced by BMP-mediated signals from epidermal ectoderm. *Cell* **82**, 969-979.
- Liem, K. F., Jr, Jessell, T. M. and Briscoe, J.** (2000). Regulation of the neural patterning activity of sonic hedgehog by secreted BMP inhibitors expressed by notochord and somites. *Development* **127**, 4855-4866.
- Lu, Q. R., Yuk, D., Alberta, J. A., Zhu, Z., Pawlitzky, I., Chan, J., McMahon, A. P., Stiles, C. D. and Rowitch, D. H.** (2000). Sonic hedgehog-regulated oligodendrocyte lineage genes encoding bHLH proteins in the mammalian central nervous system. *Neuron* **25**, 317-329.
- Mao, B., Wu, W., Li, Y., Hoppe, D., Stannek, P., Glinka, A. and Niers, C.** (2001a). LDL-receptor-related protein 6 is a receptor for Dickkopf proteins. *Nature* **411**, 321-325.
- Mao, J., Wang, J., Liu, B., Pan, W., Farr, G. H., Flynn, C., Yuan, H., Takada, S., Kimelman, D., Li, L. and Wu, D.** (2001b). Low-density lipoprotein receptor-related protein-5 binds to Axin and regulates the canonical Wnt signaling pathway. *Mol. Cell* **7**, 801-809.
- Marin, O. and Rubenstein, J. L.** (2001). A long, remarkable journey: tangential migration in the telencephalon. *Nat. Rev. Neurosci.* **2**, 780-790.
- Marin, O., Anderson, S. A. and Rubenstein, J. L.** (2000). Origin and molecular specification of striatal interneurons. *J. Neurosci.* **20**, 6063-6076.
- McCarthy, R. A. and Argraves, W. S.** (2003). Megalin and the neurodevelopmental biology of sonic hedgehog and retinol. *J. Cell Sci.* **116**, 955-960.
- McCarthy, R. A., Barth, J. L., Chintalapudi, M. R., Knaak, C. and Argraves, W. S.** (2002). Megalin functions as an endocytic sonic hedgehog receptor. *J. Biol. Chem.* **277**, 25660-25667.
- McMahon, J. A., Takada, S., Zimmerman, L. B., Fan, C. M., Harland, R. M. and McMahon, A. P.** (1998). Noggin-mediated antagonism of BMP signaling is required for growth and patterning of the neural tube and somite. *Genes Dev.* **12**, 1438-1452.
- Nery, S., Wichterle, H. and Fishell, G.** (2001). Sonic hedgehog contributes to oligodendrocyte specification in the mammalian forebrain. *Development* **128**, 527-540.
- Nykjaer, A. and Willnow, T. E.** (2002). The low-density lipoprotein receptor gene family: a cellular Swiss army knife? *Trends Cell Biol.* **12**, 273-280.
- Ohkubo, Y., Chiang, C. and Rubenstein, J. L.** (2002). Coordinate regulation and synergistic actions of BMP4, SHH and FGF8 in the rostral prosencephalon regulate morphogenesis of the telencephalic and optic vesicles. *Neuroscience* **111**, 1-17.
- Onichtchouk, D., Chen, Y. G., Dosch, R., Gawantka, V., Delius, H., Massague, J. and Niehrs, C.** (1999). Silencing of TGF-beta signaling by the pseudoreceptor BAMBI. *Nature* **401**, 480-485.
- Orentas, D. M., Hayes, J. E., Dyer, K. L. and Miller, R. H.** (1999). Sonic hedgehog signaling is required during the appearance of spinal cord oligodendrocyte precursors. *Development* **126**, 2419-2429.
- Pinson, K. I., Brennan, J., Monkley, S., Avery, B. J. and Skarnes, W. C.** (2000). An LDL-receptor-related protein mediates Wnt signalling in mice. *Nature* **407**, 535-538.
- Porter, J. A., Young, K. E. and Beachy, P. A.** (1996). Cholesterol modification of hedgehog signaling proteins in animal development. *Science* **274**, 255-259.
- Roessler, E., Belloni, E., Gaudenz, K., Jay, P., Berta, P., Scherer, S. W., Tsui, L. C. and Muenke, M.** (1996). Mutations in the human Sonic Hedgehog gene cause holoprosencephaly. *Nat. Genet.* **14**, 357-360.
- Rowitch, D. H., S-Jacques, B., Lee, S. M., Flax, J. D., Snyder, E. Y. and McMahon, A. P.** (1999). Sonic hedgehog regulates proliferation and inhibits differentiation of CNS precursor cells. *J. Neurosci.* **19**, 8954-8965.
- Saito, A., Pietromonaco, S., Loo, A. K. and Farquhar, M. G.** (1994). Complete cloning and sequencing of rat gp330/"megalin," a distinctive member of the low density lipoprotein receptor gene family. *Proc. Natl. Acad. Sci. USA* **91**, 9725-9729.
- Sasai, Y. and de Robertis, E. M.** (1997). Ectodermal patterning in vertebrate embryos. *Dev. Biol.* **182**, 5-20.
- Schneider, R. A., Hu, D., Rubenstein, J. L., Maden, M. and Helms, J. A.** (2001). Local retinoid signaling coordinates forebrain and facial morphogenesis by maintaining FGF8 and SHH. *Development* **128**, 2755-2767.
- Sussel, L., Marin, O., Kimura, S. and Rubenstein, J. L.** (1999). Loss of Nkx2.1 homeobox gene function results in a ventral to dorsal molecular respecification within the basal telencephalon: evidence for a transformation of the pallidum into the striatum. *Development* **126**, 3359-3370.
- Tallquist, M. D. and Soriano, P.** (2000). Epiblast-restricted Cre expression in MORE mice: a tool to distinguish embryonic vs. extra-embryonic gene function. *Genesis* **26**, 113-115.
- Timmer, J. R., Wang, C. and Niswander, L.** (2002). BMP signaling patterns the dorsal and intermediate neural tube via regulation of homeobox and helix-loop-helix transcription factors. *Development* **129**, 2459-2472.
- Trommsdorff, M., Gotthardt, M., Hiesberger, T., Shelton, J., Stockinger, W., Nimpf, J., Hammer, R. E., Richardson, J. A. and Herz, J.** (1999). Reeler/Disabled-like disruption of neuronal migration in knockout mice lacking the VLDL receptor and ApoE receptor 2. *Cell* **97**, 689-701.
- Wallis, D. E. and Muenke, M.** (1999). Molecular mechanisms of holoprosencephaly. *Mol. Genet. Metab.* **68**, 126-138.
- Wallis, D. E., Roessler, E., Hehr, U., Nanni, L., Wiltshire, T., Richieri-Costa, A., Gillissen-Kaesbach, G., Zackai, E. H., Rommens, J. and Muenke, M.** (1999). Mutations in the homeodomain of the human SIX3 gene cause holoprosencephaly. *Nat. Genet.* **22**, 196-198.
- Wehrli, M., Dougan, S. T., Caldwell, K., O'Keefe, L., Schwartz, S., Vaizel-Ohayon, D., Schejter, E., Tomlinson, A. and DiNardo, S.** (2000). arrow encodes an LDL-receptor-related protein essential for Wingless signalling. *Nature* **407**, 527-530.
- Willnow, T. E., Goldstein, J. L., Orth, K., Brown, M. S. and Herz, J.** (1992). Low density lipoprotein receptor-related protein and gp330 bind similar ligands, including plasminogen activator-inhibitor complexes and lactoferrin, an inhibitor of chylomicron remnant clearance. *J. Biol. Chem.* **267**, 26172-26180.
- Willnow, T. E., Hilpert, J., Armstrong, S. A., Rohmann, A., Hammer, R. E., Burns, D. K. and Herz, J.** (1996). Defective forebrain development in mice lacking gp330/ megalin. *Proc. Natl. Acad. Sci. USA* **93**, 8460-8464.
- Wilson, S. W. and Houart, C.** (2004). Early steps in the development of the forebrain. *Dev. Cell.* **6**, 167-181.
- Zheng, G., Bachinsky, D. R., Stamenkovic, I., Strickland, D. K., Brown, D., Andres, G. and McCluskey, R. T.** (1994). Organ distribution in rats of two members of the low-density lipoprotein receptor gene family, gp330 and LRP/alpha 2MR, and the receptor-associated protein (RAP). *J. Histochem. Cytochem.* **42**, 531-542.